

# Observations of Compact X-Ray Sources

Y. Tanaka

Institute of Space and Astronautical Science,  
4-6-1 Komaba, Meguro-ku, Tokyo 153, Japan

This paper reviews the present status of observations of compact X-ray sources with emphasis on the aspects related to radiation hydrodynamics, based on the recent observational results, in particular those from the Japanese X-ray astronomy satellite Tenma. The main feature of Tenma is a large-area gas scintillation proportional counters (GSPC) with energy resolution twice that of ordinary proportional counters, which can yield information on energy spectrum superior in quality to previous results. We shall deal here only with those galactic X-ray sources in which the compact object is a neutron star or possibly a black hole, and exclude white dwarf sources.

## I. Accretion-Powered X-Ray Emission

There exist more than one hundred bright X-ray sources in our galaxy in the luminosity range  $10^{36}$ - $10^{38}$  ergs/sec. They are most probably binaries involving a neutron star or, in some cases, possibly a black hole. The high luminosities of these sources are explained in terms of the large gravitational energy release by matter accreting from the companion star to the compact object.

These X-ray sources can be divided into two classes with respect to their companion stars:

- (1) Massive binaries; sources with massive companions, mostly O,B stars, which are distributed along the galactic arms. Hence, these sources are considered to be young ( $10^6$ - $10^7$  years) systems.
- (2) Low-mass binaries; companions are low-mass stars of  $1M_{\odot}$  or smaller. Sources in this class are distributed preferentially near the galactic center, and are often found in globular clusters. These facts indicate that these sources are old systems.

Most of the massive binary sources manifest themselves as X-ray pulsars. Whereas, with only one or two exceptions (X1627-67 and possibly GX1+4), low-mass binary sources are not X-ray pulsars. On the other hand, many of the low-mass binary sources produce X-ray bursts. As a matter of fact, no X-ray pulsar produces bursts, and no burst source pulsates. This clear distinction is considered to come from a large difference in the magnetic field strengths of the neutron stars. Young neutron stars possess strong magnetic fields of the order of  $10^{12}$  Gauss, whereas the field would probably be much weaker for old neutron stars.

In addition, there are several sources in which the compact object is suspected to be a black hole. These "black-hole candidates" are discussed separately.

### I-1. Strongly Magnetized Neutron Stars; X-Ray Pulsars

We shall deal with binary X-ray pulsars in this section. There are 26 binary X-ray pulsars known to date, including SMC X-1 and LMC X-4. The observed pulse periods are distributed from 69 msec to 894 sec, ranging over four orders of magnitude. For a strongly magnetized neutron star in X-ray pulsars, accreting matter is stopped once at the Afven surface and then funnelled into the magnetic poles. Unfortunately, we do not yet well understand the basic physics involved in the energy release of accreting matter on the magnetic poles and subsequent radiation transport through a highly magnetized

plasma. These are the processes which eventually form the observed pulse profiles and energy spectra characteristic of X-ray pulsars. For general reviews of binary X-ray pulsars, see, e.g., [1][2].

### (i) Pulse Profile

The pulse profile of each pulsar reflects the pattern of X-ray beams emanating from the magnetic poles. Whether they are pencil beams or fan beams is not yet certain. Figure 1 shows examples of average pulse profiles of several X-ray pulsars [1]. Qualitatively, the pulse profile and its energy dependence are explained in terms of the anisotropy of Thomson scattering in a highly magnetized plasma, determined by the angle between the line of sight and the momentary direction of the magnetic dipole axis ([1][2] and references therein). There is a clear tendency for the profile to become simpler at higher energies.

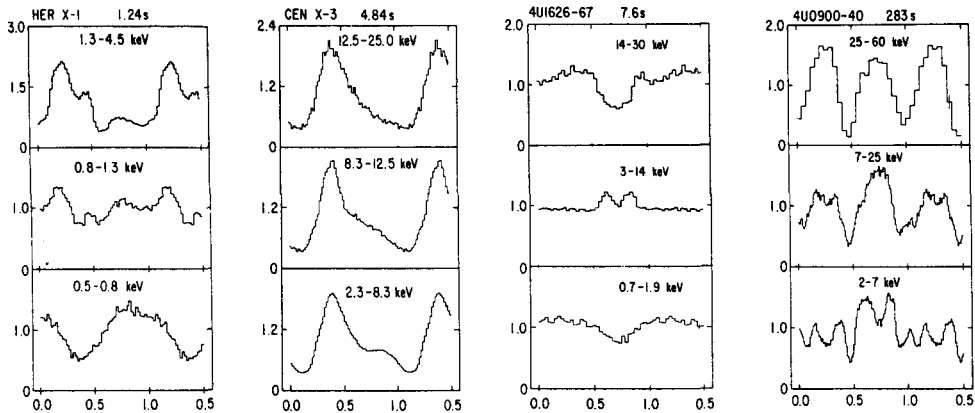


Fig. 1. Average profiles of four X-ray pulsars

The pulse profile can exhibit large changes from time to time, as shown for example for Vel X-1 in Fig. 2. For many pulsars, one complete pulse comprises a main pulse and an intermediate pulse, which are attributed to the two poles respectively. An interesting phenomenon was observed in Vel X-1, as shown in Fig. 3, when only the main pulse flared up while the intermediate pulse remained almost unchanged, suggesting that the accretion onto only one pole was suddenly enhanced.

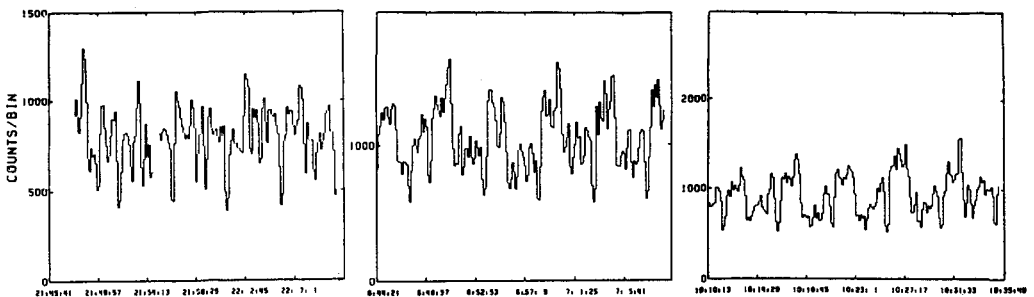


Fig. 2. Variation of the pulse profile of Vel X-1 observed from Tenma

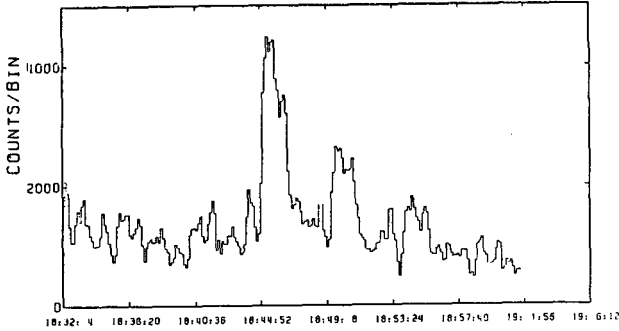


Fig. 3. Sudden enhancement of main pulses of Ve1 X-1

More dramatically, the pulsation can stop suddenly. Figure 4a shows such an event observed from Ve1 X-1 [3]. Figure 4b shows a qualitatively different event for GX301-2 in which pulse modulation disappears for some time while a steady component remains [4]. A similar case was also observed from Cen X-3. These unusual behaviors are not explained in terms of conventional models of X-ray pulsars.

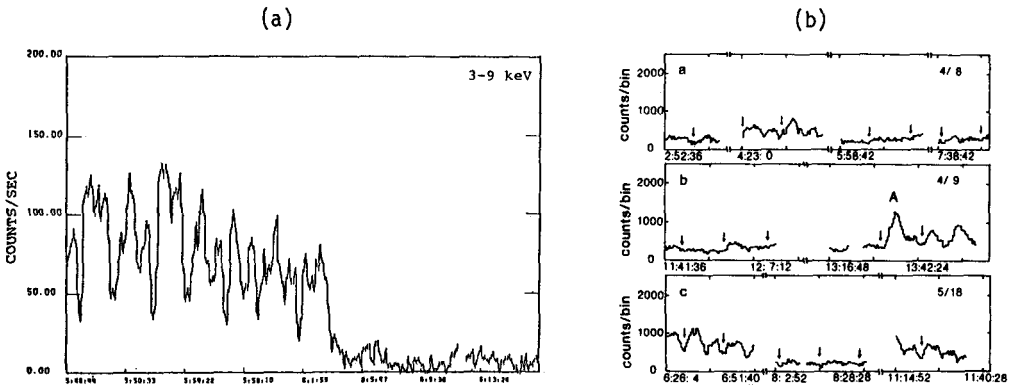


Fig. 4. Disappearance of pulsations for (a) Ve1 X-1, and (b) GX301-2

(ii) Energy Spectrum

Energy spectra of several X-ray pulsars observed from Tenma are shown in Fig. 5. These spectra are generally represented by a power law with a steep fall-off starting between 10 and 20 keV. The power-law indices of the photon number spectrum are distributed in the range 0.5-1.5. It has been unclear whether the high-energy fall-off is of thermal origin (the electron temperature above the magnetic poles) or it reflects cyclotron absorption. High-quality spectra obtained with the Tenma GSPC allow us to study the nature of this high-energy fall-off at least empirically.

It is found that the following two model spectra satisfactorily reproduce the form of the high-energy fall-off:

(a) Fermi-Dirac type distribution;  $1/[1+\exp(E-E_C)/E_F]$  and

(b) cyclotron resonance absorption;  $\exp[-KE^2/(E-E_H)^2]$ ,

both multiplied by a power law  $E^{-\alpha}$ . The results of fittings to the observed spectra from Tenma are shown in Table 1. The fitting was performed in the range above 7 keV.

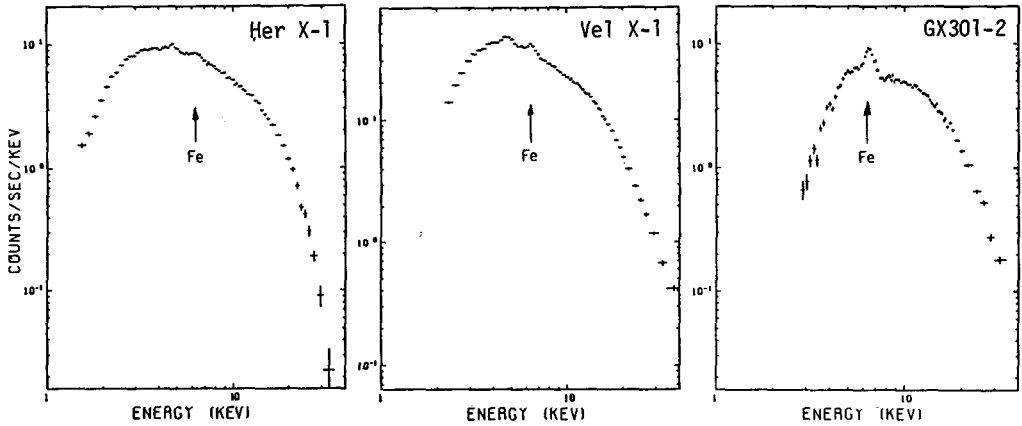


Fig. 5. Observed spectra of three X-ray pulsars (Not deconvolved for the detector response. The feature at 4.8 keV in all GSPC spectra is an instrumental artifact.)

Table I. Spectral parameters of X-ray pulsars (Errors are given in parentheses.)

NAME	PERIOD(S)	FERMI-DIRAC CUT-OFF				CYCLOTRON ABSORPTION			
		$\alpha$	$E_C$ (KEV)	$E_F$ (KEV)	RED. $\chi^2$	$\alpha$	$E_H$ (KEV)	K	RED. $\chi^2$
HER X-1	1.24	0.95(.03)	24.7(.3)	2.5(.3)	1.76	0.89(.04)	36.(2.)	0.1(.7)	2.39
X0331+53	4.38	0.42(.05)	20.6(.6)	4.1(.3)	1.55	0.32(.06)	64.(11.)	4. (2.)	1.90
CEN X-3	4.83	0.41(.11)	8. (2.)	5.5(.3)	1.96				
X1626-67	7.67	1.28(.09) 0.32(.11)	19.2(.7) 28. (1.)	2.4(.8) 1. (1.)	1.37 2.22	1.2 (.1) 0.1 (.1)	31.(9.) 29.(1.)	0.3(.5) 0.004(.002)	1.28 1.24
X1657-41	37.9	1.51(.04)	0.2(.1)	12.5(.2)	7.50				
X1700-37	67.4	1.63(.02)	----	----	1.11				
X0535+26	103.	1.28(.03)	27. (4.)	22.(1.)	2.90				
VELA X-1	283.	0.76(.14)	24. (4.)	8.(2.)	1.14	0.77(.07)	124.(60.)	11.(13.)	1.17
X1907+09	438.	1.60(.05)	----	----	2.24				
X1538-52	530.	0.95(.13)	18.2(.5)	1.9(.5)	1.68	0.75(.18)	30.(6.)	0.3(.5)	1.87
GX301-2	700.	0.76(.13)	26. (2.)	6.(2.)	1.21				

If the fall-off were of thermal origin,  $E_F$  is expected to be approximately one third of  $E_C$ , for the fitting with Fermi-Dirac formula. However, one notices that for several pulsars, Her X-1, X0331+53, X1627-67 and X1538-52,  $E_F$  is much smaller than one-third of  $E_C$ , a fall-off which appears too sharp to be of thermal origin.

Cyclotron resonance absorption model can equally well explain the shape of the fall-off, though there is as yet no convincing evidence that it is indeed the case. The determined  $E_H$  values listed in Table I correspond to several times  $10^{12}$  G. Of particular interest is the case of X1627-67 which exhibits a significant change of fall-off according to the pulse phase, as shown in Fig. 6. As seen in Table I,  $E_C$  moves from 19 keV to 28 keV, whereas  $E_H$  remains the same within the uncertainties.

So far the most prominent spectral feature is the apparent cyclotron line(s) detected from Her X-1 [5], as shown in Fig. 7. If this 53 keV peak is interpreted to be the emission line due to the Landau level transition, the magnetic field is estimated to be  $5.3 \times 10^{12}$  G. If, on the other hand, the structure were due to cyclotron resonance absorption, the field strength would be  $3.8 \times 10^{12}$  G.

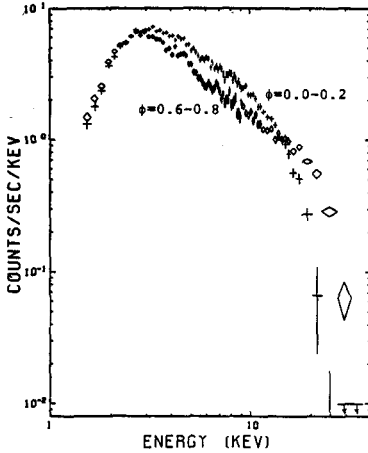


Fig. 6. Spectra of X1627-67 at two pulse-phases

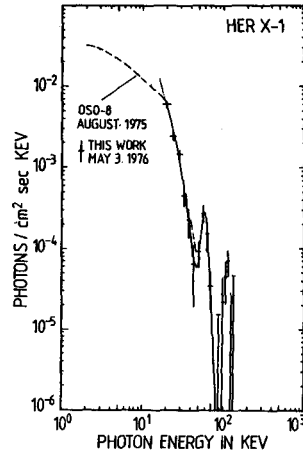


Fig. 7. Cyclotron features of Her X-1

### (iii) Iron Emission Line

X-ray pulsar spectra commonly reveal intense iron emission lines at 6.4 keV, as seen in Fig. 5. Exceptions are X1627-67 (low-mass X-ray pulsar) and X0331+53 (recurrent transient), from which no significant iron line is observed. This distinction is an interesting problem by itself. The line energy of 6.4 keV implies an ionization state of iron probably lower than Fe XX, and a much lower ionization state than FeXX is inferred from the observed iron K-absorption edges, significantly observed for Vel X-1 [6] and GX301-2. This supports a fluorescence origin of the emission line from relatively cool matter which is illuminated by X-rays. The iron line has so far been considered to be emitted from matter that covers the Alfvén shell [7]. However, as discussed below, the situation does not seem to be so simple.

We performed a Monte Carlo calculation for the fluorescence iron line emission from neutral matter that surrounds the neutron star spherically [6][8]. The line intensity is calculated as a function of absorbing column  $N_H$ . For the continuum X-rays from the central source, the observed phase-averaged spectrum after correction for absorption is employed. This model corresponds to the case of fan beams such that the phase-averaged flux is isotropic. The apparent fluorescence efficiency (the ratio of the emerging iron line to the source intensity above 7 keV) increases with  $N_H$ , until it reaches a maximum for several times  $10^{23}$  H atoms/cm<sup>2</sup>. It then decreases against  $N_H$ , because absorption predominates production of the line.

We find that the observed values are often significantly greater than expected from the model. In Fig. 8, the observed efficiency for Vel X-1 is compared with the Monte Carlo result [6]. The observed values are much greater than expected for  $N_H$ -values smaller than  $10^{23}$  H atoms/cm<sup>2</sup>, and is essentially constant independent of  $N_H$ . The lack of  $N_H$ -dependence implies that the absorption column on the line of sight does not represent the amount responsible for the line production. Yet, the observed efficiency is near the maximum value expected for a  $4\pi$  coverage of the central source with an absorption column greater than  $10^{23}$  H atoms/cm<sup>2</sup>, which is in contradiction with the observed result.

Another important piece of information obtained from at least two pulsars, Vel X-1 and GX301-2, is that the iron line intensity does not pulsate as shown in Fig. 9 [6]. These two facts together can be explained if, instead of fan beams, most of the X-ray emission were confined in pencil beams which sweep around outside the line of sight. In this case, the beam flux could be much more intense than we actually observe. When sufficient amount of matter were sustained over the poles, it would always receive the pencil beams, whereby resulting in the absence of pulsation of the iron line [6].

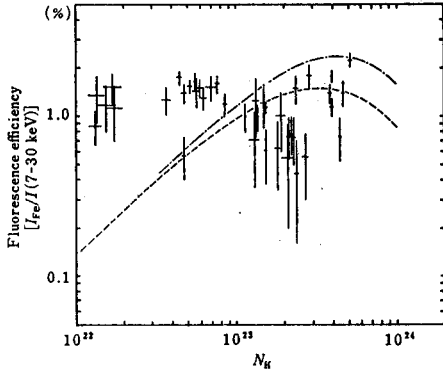


Fig. 8. Apparent fluorescence efficiency observed (Vel X-1) and computed vs.  $N_H$

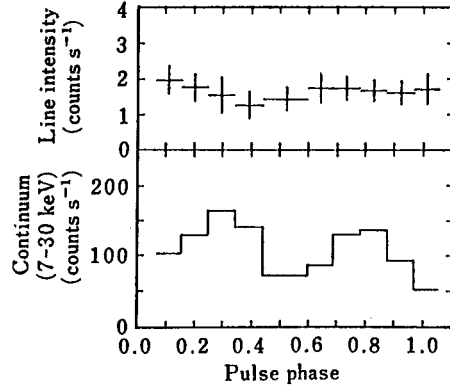


Fig. 9. Iron line and continuum intensities as functions of pulse phase

I-2. Weakly Magnetized Neutron Stars

(i) Continuum Spectrum

The nature of the spectrum of non-pulsating low-mass binary X-ray sources has not yet been well understood. Accreting matter is considered to form an accretion disk around a neutron star. If magnetic fields are sufficiently weak, the accretion disk will extend close to the neutron star surface. According to the standard model (e.g., [9] and references therein), the accretion disk outside a certain inner radius will be optically thick. Inside this radius, radiation pressure dominates and the disk inflates to form an optically-thin torus. Matter circulating along Keplerian orbits gradually falls inward, and the released gravitational energy is equipartitioned between thermal and rotational energies. The thermal energy is efficiently radiated away from the optically-thick disk. However, the emissivity of the inner optically-thin region is very low so that the energy released in this region will be transported together with the rotational energy onto the neutron star surface. Thus, one expects two separate emission regions; (a) the optically-thick accretion disk, and (b) the neutron star surface.

The spectrum from the optically-thick accretion disk,  $F_d(E)$ , will be given by the following "multi-color" blackbody spectrum;

$$F_d(E) = (\cos\theta/D^2) \int_{r_{in}}^{\infty} 2\pi r B(E,T(r)) dr \tag{1}$$

where  $B(E,T)$  is the Planck distribution with temperature  $T$ ,  $\theta$  the inclination angle of the disk,  $D$  the source distance and  $r_{in}$  the inner boundary radius of the optically-thick disk. Since  $T$  is proportional to  $r^{-3/4}$  in the optically-thick disk, the above equation is rewritten as

$$F_d(E) = (8\pi \cos\theta/3D^2) r_{in}^2 \int_0^{T_{in}} (T/T_{in})^{-1/3} B(E,T) dT/T_{in} \tag{2}$$

where  $T_{in}$  is the temperature at the inner boundary  $r_{in}$ .

On the other hand, the neutron star surface will emit blackbody radiation and the spectrum is expressed by

$$F_b(E) = (S'/D^2) B(E,T_b) \tag{3}$$

where  $S'$  is the projected area of the emitting surface.

Typically, low-mass binary sources exhibit intensity variations of a factor of two to three on time scales of the order of an hour. It has often been noted during such intensity variations that the spectrum hardens when the intensity increases. We examined this behavior for several bright sources observed from Tenma [10].

We compared the spectra when the intensity was high with those in adjacent periods of lower intensity. Examples are shown in Fig. 10. The difference between high- and low-intensity spectra is always expressed very well by a single blackbody spectrum with  $kT$  of approximately 2 keV for all sources examined, except for a slight but significant excess above 10 keV. This high-energy excess is considered to be due to Comptonization, which will be discussed later. Furthermore, the blackbody temperature is found to be fixed for a given source. Thus, the hardening of the spectrum is caused by an intensity increase in this blackbody component. This result strongly suggests that the "2-keV blackbody" is intrinsic to the source.

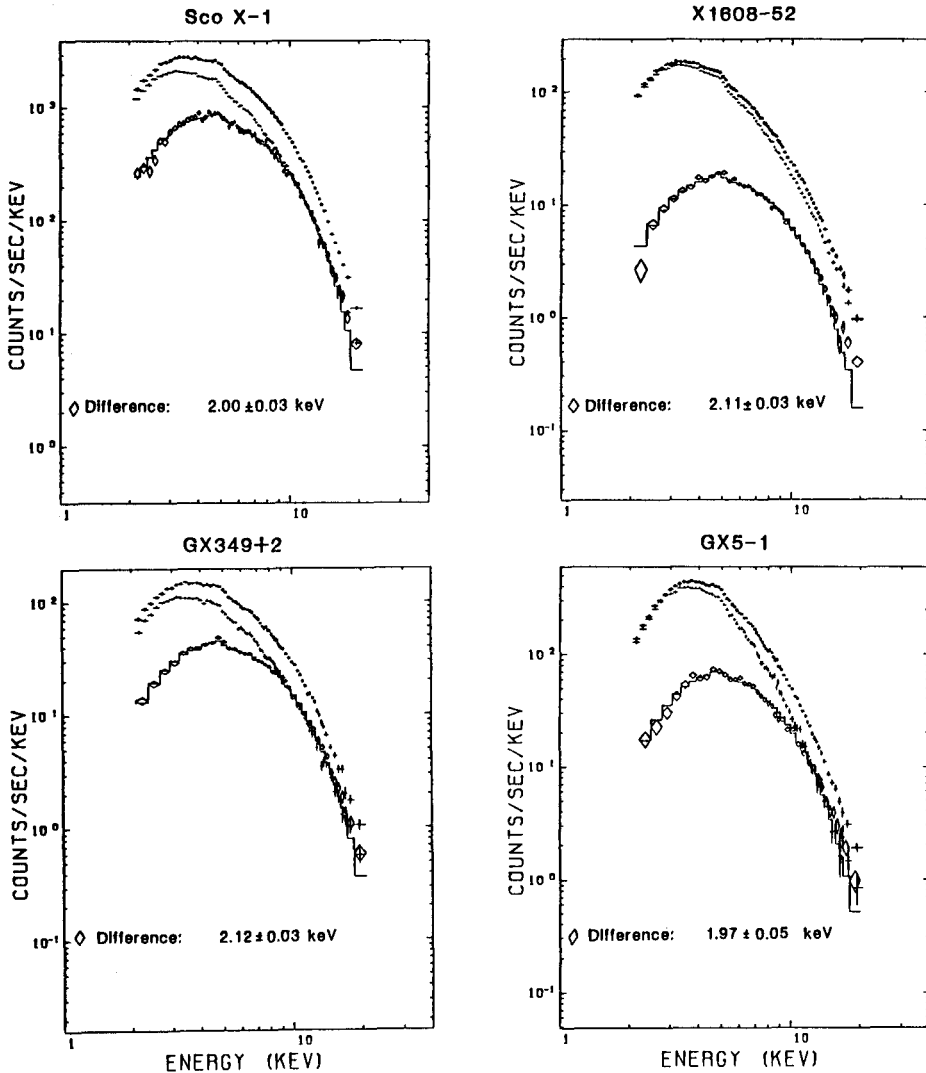


Fig. 10. Spectra of four low-mass binary sources at high- and low-intensity levels, and their differences. Histograms show the best-fit blackbody spectra to the differences.

Then, the observed spectrum can be decomposed into two spectral components; a 2-keV blackbody component and a softer component, as shown in Fig. 11. The softer component for a source is found always to have a fixed form, and those for different sources are similar to each other. Again, this softer component is shown to be a real constituent of the spectrum. This is demonstrated by the spectra observed during the intensity dips of GX5-1. The light curves in Fig. 12(a) show some of these dips. The observed spectrum during a dip, shown in Fig. 12(b), is found to be nearly identical to the softer component derived from the spectral decomposition in Fig. 11. Thus, the intensity dip of GX5-1 is understood as being due to a sudden disappearance of the 2-keV blackbody component, hence the softer component alone shows up.

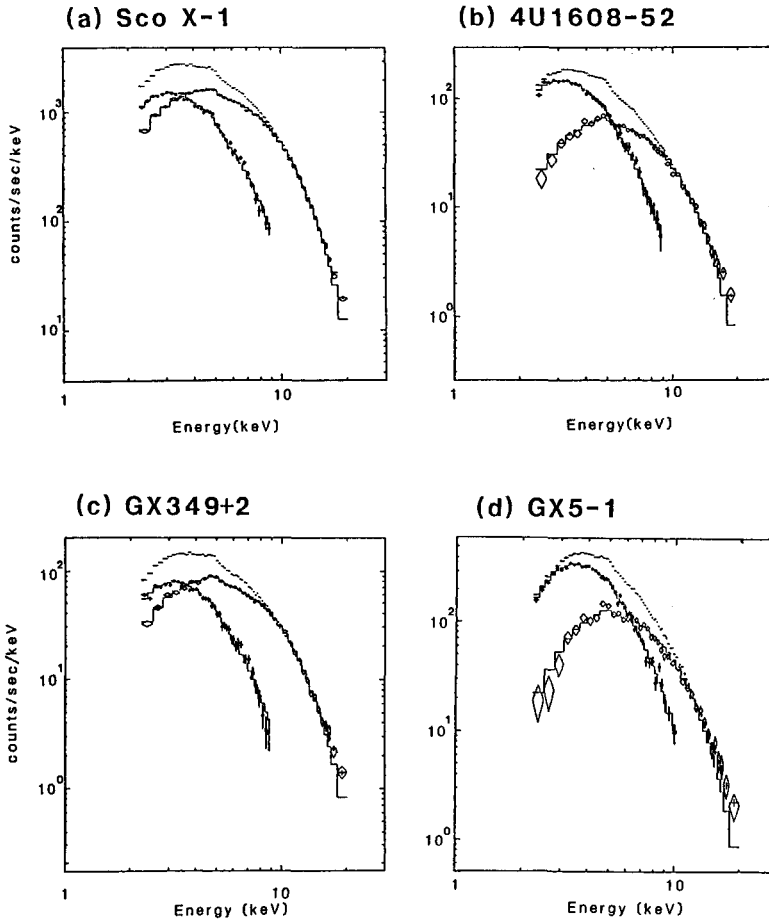


Fig. 11. Decomposition of the observed spectra into a 2-keV blackbody and a softer components. Histograms are the best-fit spectra of the form given by Eq. 2 and 3.

The observed spectrum of the softer component is found to be well expressed by that expected from an optically-thick accretion disk given by Eq. 2. The temperature at the inner disk edge  $kT_{in}$  is typically 1.3–1.4 keV for the luminous group of sources. From these results, it is most plausible to interpret the softer component as the emission from an optically-thick accretion disk around the neutron star and the 2-keV component as that from the neutron star envelope [10].

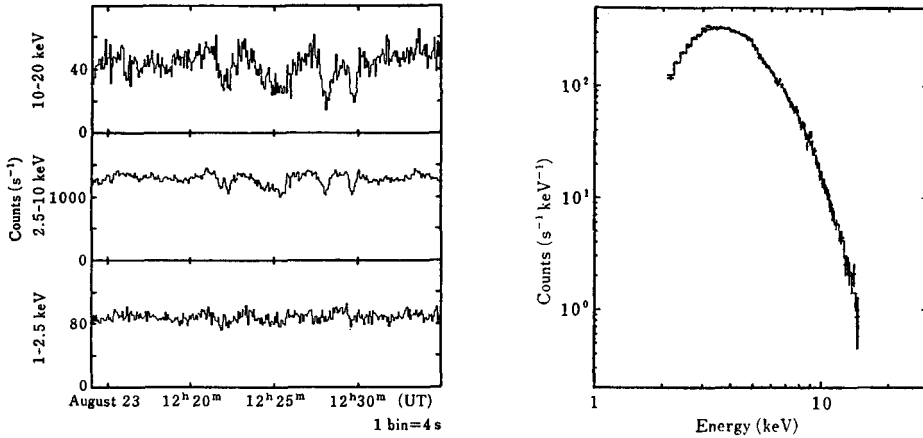


Fig. 12. (a) Light curves of GX5-1 including dips, and (b) the spectrum during a dip

Figure 13 shows the light curves of the 2-keV component and the softer component for four luminous sources. There is a striking difference in the time-variability between these two components: The 2-keV component is highly variable on a time-scale of an hour or shorter, whereas the softer component is remarkably stable. This may indicate that the accretion rate itself remains fairly constant as implied by the stable disk emission, but that the accretion flow inside  $r_{in}$  onto the neutron star is unstable due to some as yet unknown reason. This would imply a discontinuity of the accretion flow at the inner disk boundary, hence a temporary storage of matter in the disk may occur.

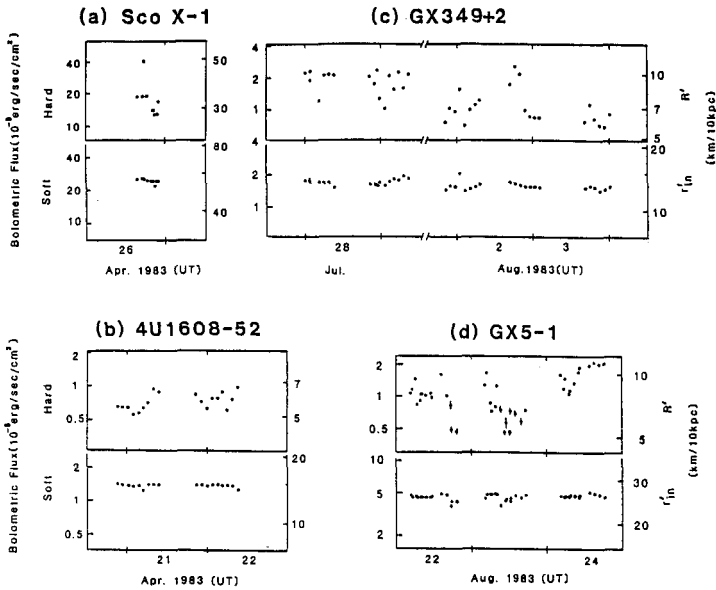


Fig. 13. Time variations of the 2-keV (hard) and softer components for four sources

Having identified the spectral components, we can determine the parameters for each low-mass binary source observed. In addition, as mentioned earlier, a high-energy tail above 10 keV is frequently observed in the spectra of low-mass binary sources, most probably due to Comptonization in an optically-thin hot plasma surrounding the neutron stars. Recently, Comptonization for small optical depths was solved analytically by ITOH [11] and NISHIMURA et al. [12]. We employ their result and determine the Comptonization  $y$ -parameter,  $4kT_e/mc^2$ . Table II lists all spectral parameters for thirteen low-mass binary sources that were observed from Tenma [13]. Most of the sources have blackbody temperatures  $kT_b$  between 1.7 and 2 keV and temperatures at the inner disk boundary  $kT_{in}$  between 0.9 and 1.4 keV. There is a tendency for both  $T_b$  and  $T_{in}$  to be smaller and  $y$  larger respectively for sources of lower brightness. Among the sources in Table II, no X-ray burst has been observed from Sco X-1, Cyg X-2, GX5-1, and GX349+2. This might be related to the fact that these sources are probably more luminous than the others. Other sources in Table II are known to produce bursts.

Table II. Spectral parameters for thirteen low-mass binary sources observed from Tenma

Source	Flux(2-20keV) ( $10^{-9}$ erg/cm $^2$ s)	$T_{in}$ (keV)	$T_b$ (keV)	$y$	Reduced $\chi^2$ (d.o.f: 51)
Sco X-1	260	$1.58^{+0.72}_{-0.33}$	$1.91^{+0.50}_{-0.16}$	$0.16 \pm 0.04$	1.28
GX5-1	23	$1.32^{+0.18}_{-0.10}$	$1.81^{+0.15}_{-0.11}$	$0.12 \pm 0.02$	0.69
GX349+2	18	$1.08^{+0.17}_{-0.15}$	$1.73^{+0.07}_{-0.05}$	$0.21 \pm 0.02$	1.30
X1608-52	11	$1.34^{+0.24}_{-0.13}$	$1.91^{+0.03}_{-0.12}$	$0.22 \pm 0.04$	1.59
"	2.7	$0.78^{+0.06}_{-0.06}$	$1.56^{+0.06}_{-0.05}$	$0.29 \pm 0.02$	1.20
"	1.5	$0.77^{+0.12}_{-0.10}$	$1.38^{+0.17}_{-0.13}$	$1.2 \pm 0.1$	1.06
Cyg X-2	9.0	$1.23^{+0.42}_{-0.23}$	$1.82^{+0.50}_{-0.24}$	$0.3 \pm 0.2$	1.04
Ser X-1	3.9	$1.23^{+0.28}_{-0.23}$	$1.82^{+0.40}_{-0.20}$	$0.24 \pm 0.05$	1.20
NGC6624	3.7	$1.23^{+0.18}_{-0.12}$	$2.05^{+0.14}_{-0.10}$	$0.17 \pm 0.04$	0.95
X1735-44	2.2	$0.94^{+0.14}_{-0.04}$	$1.82^{+0.13}_{-0.03}$	$0.37 \pm 0.02$	1.03
X1636-53	2.0	$0.94^{+0.04}_{-0.06}$	$1.76^{+0.03}_{-0.04}$	$0.34 \pm 0.02$	1.10
"	1.2	$0.69^{+0.14}_{-0.09}$	$1.58^{+0.18}_{-0.08}$	$0.45 \pm 0.01$	1.02
X1728-33	2.6	$0.77^{+0.12}_{-0.06}$	$1.63^{+0.07}_{-0.06}$	$0.52 \pm 0.02$	0.90
"	2.2	$0.66^{+0.07}_{-0.06}$	$1.41^{+0.05}_{-0.04}$	$0.75 \pm 0.02$	1.01
X1905+00	0.89	$0.55^{+0.14}_{-0.14}$	$1.27^{+0.21}_{-0.16}$	$0.5 \pm 0.2$	1.74
X1254-69	0.55	$0.78^{+0.25}_{-0.11}$	$1.40^{+0.15}_{-0.08}$	$0.5 \pm 0.2$	1.61
X0614+09	0.38	$0.59^{+0.16}_{-0.16}$	$1.26^{+0.16}_{-0.16}$	$< 0.30$	0.78

## (ii) Luminosity-Related Change of Spectrum

Here, we show that the spectrum of a low-mass binary source changes its shape substantially with a change in luminosity (accretion rate). Figure 14 shows such an example observed for X1608-52 [13]. As the luminosity goes down, the high-energy tail becomes more and more pronounced and consequently the whole spectrum approaches a power-law spectrum.

This result can be explained in terms of changes in the two spectral components and the Compton optical depth, discussed above. The corresponding spectral parameters as functions of the observed flux are shown in Fig. 15. It is clearly seen that, as intensity decreases, both  $T_b$  and  $T_{in}$  become lower, at the same time that the Compton  $y$ -parameter increases. This result may indicate that the optically-thin hot region surrounding the neutron star extends when the accretion rate is reduced. Similar cases were also observed for X1728-34 and X1636-53 (see Table II).

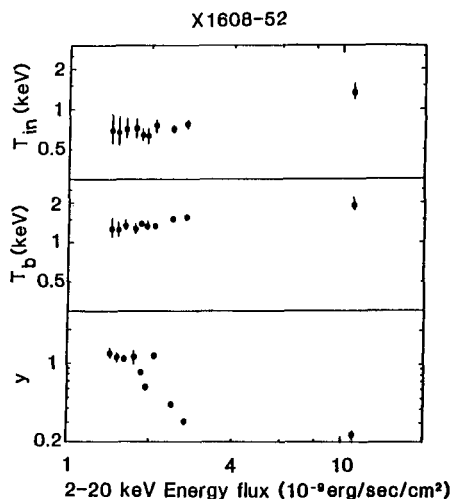
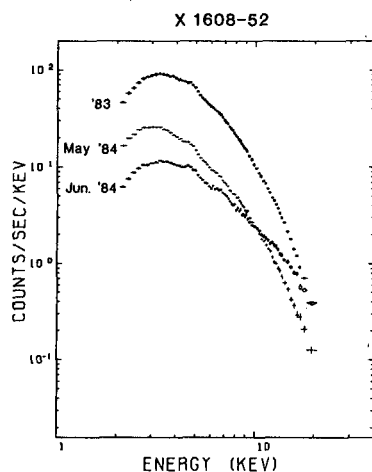


Fig. 14. Change of spectrum of X1608-52

Fig. 15. Spectral parameters vs. flux

The above result clearly demonstrates that the spectrum of a low-mass binary source can undergo a dramatic change from a thermal type spectrum to a power-law type spectrum depending on the accretion rate. This fact may have important bearing on the two spectral states exhibited by some black-hole candidates (see Section I-4).

## (iii) Iron Emission Line

A weak emission line of iron has been detected from several low-mass binary sources. The energy of the line is found to be 6.7 keV, indicating the emission from helium-like ions. This is in contrast to the 6.4-keV line observed from X-ray pulsars. The iron lines observed from Sco X-1 and X1608-52 are shown in Fig. 16 [14].

The origin of this 6.7-keV line is an interesting problem. One possibility is to assume that the line is due to thermal emission from an optically-thin plasma. For this, the line energy of 6.7 keV requires a temperature of  $(2-4) \times 10^7$  K (e.g., [15]). However, there is a problem for such an optically-thin thermal plasma to be present at these temperatures [14]. Rather, it would be more plausible that the line is of fluorescence origin from an X-ray-ionized plasma formed on the outer accretion disk by irradiation from the central source [14][16]. In this case, a close correlation between the line and continuum intensities is expected. However, the iron line intensity observed from Sco X-1 remained constant in an event when the continuum changed by a factor of two. So, the origin of the 6.7 keV line is not entirely clear yet.

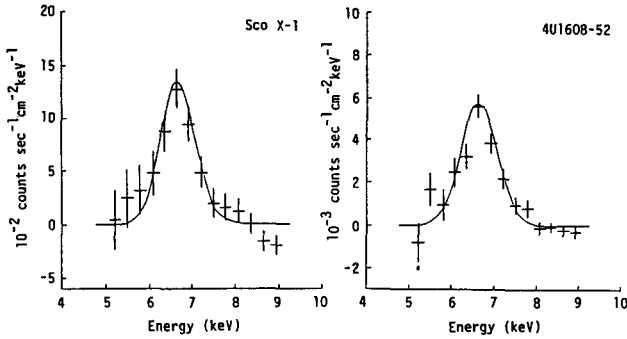


Fig. 16. Emission lines of iron at 6.7 keV observed from Sco X-1 and X1608-52 (Tenma)

### I-3. An Exotic Accretion; the Rapid Burster

In 1976, a peculiar X-ray source was discovered by LEWIN et al. [17] which produced rapidly repetitive bursts. They named this source the Rapid Burster. The Rapid Burster is unique in many respects and is still the single source of its kind in our galaxy. The Rapid Burster is located in the globular cluster Liller 1 near the galactic center. It is a recurrent transient with an apparent period of roughly six months, although the recurrence is not reliable. The rapid burst activity typically lasts a few weeks. We observed its activity three times, once from Hakucho and twice from Tenma.

The rapid bursts are most probably due to chopped accretion flow caused by some instabilities [18]. Therefore, they are the manifestation of an intermittent gravitational energy release. HOFFMAN et al. [18] designated this type of burst Type II, as opposed to Type I bursts which are considered to be nuclear energy release on the neutron star surface. We shall discuss Type I bursts separately in Section II. The Rapid Burster produces Type I bursts as well, hence it is believed to be an accreting neutron star.

The Rapid Burster displays various modes of activity. One extreme is a fairly regular series of short, spiky bursts, and another extreme is a train of long, flat-topped bursts [19]. A variety of rapid burst profiles is shown in Fig. 17 [20]. The burst duration spans a wide range from a few seconds to more than 10 minutes. Large bursts tend to saturate causing a flat-top profile. However, the saturation level is not constant but varies by factors as large as four. The cause of this luminosity saturation at various levels is not understood yet.

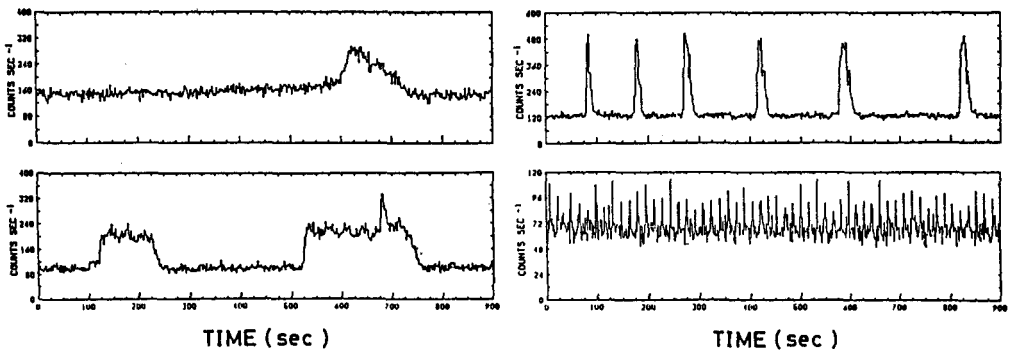


Fig. 17. Rapid burst profiles observed from Tenma

Remarkably, the rapid bursts exhibit characteristics of a relaxation oscillator [17]; the larger the size (integrated flux) of a burst, the longer in proportion to the size is the waiting time to the next burst (see, for example, the right top panel of Fig. 17). This distinct feature would imply the presence of a reservoir of fixed capacity. Then, the bursts of durations as long as 10 minutes imply that the reservoir can store at least  $10^{21}$  grams of matter [19]. It is likely that the accretion disk itself serves as this reservoir. However, what mechanism triggers and stops the accretion flow is entirely unknown.

The energy spectra of the rapid bursts are best represented by blackbody spectra with a significant hard tail. An example is shown in Fig. 18 [21]. From the observed blackbody temperature, the apparent size of the blackbody is derived for a given distance. It is worth mentioning that the blackbody temperature remains essentially constant throughout a burst and the decay of burst is due to a diminishing area of emission with time. This is in contrast to the behavior of Type I bursts in which the blackbody temperature decreases through the burst decay, whereas the blackbody size remains constant (see Section II).

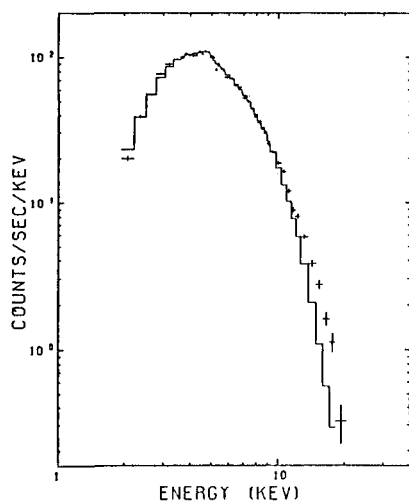


Fig. 18. Spectrum of a rapid burst  
Histogram is the best-fit blackbody  
spectrum.

For the rapid bursts, the blackbody temperature and apparent blackbody radius vary from burst to burst in the range 1.6–2.0 keV and 8–15 km for 10 kpc distance, respectively [21]. On the other hand, Type I bursts from the same source invariably give an apparent blackbody radius of 7 km [21], which is, according to the discussions in Section II, considered to represent the radius of the neutron star (see, however, the discussion in Section II-1). The above facts indicate that the emission region of the rapid bursts is optically thick and more extended than the neutron star surface, perhaps surrounding the neutron star. The structure of the emitting region during a rapid burst appears to be distinctly different from that of persistent low-mass binary sources discussed previously. The spectrum of a rapid burst is similar to the 2-keV blackbody component which is interpreted to come from a fraction of the neutron star surface. Whereas, a rapid burst is emitted from a more extended region than the size of the neutron star. The spectrum of a rapid burst also lacks the softer component expected from an optically-thick accretion disk. This suggests that the optically-thick disk stops at a distance farther than  $10^2$  km from the neutron star, so that the emission falls below the X-ray energy band. This would occur if a magnetic field of the order of  $10^9$  G were present (which is still not strong enough to make it a pulsar).

The rapid bursts exhibit various time structures of interest. In two long, flat-topped bursts, quasi-periodic oscillations at about 2 Hz were observed from Hakucho [22]. Obviously, this periodicity is not that of the neutron star rotation, because it changed slightly with time.

A multi-peaked structure is commonly noted in the decay of rapid bursts. Figure 19 displays several bursts of different durations. The structure is not that of a simple damping oscillation, but more complex. Clearly, the time scale of the decay structure depends on the burst duration; the longer the burst duration, the slower is the excursion of the decay structure. A striking similarity is noticed in the shape of the decay structure between bursts, except for the time scale.

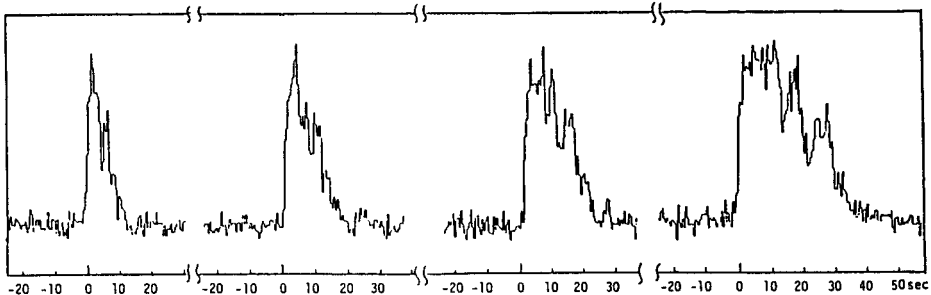


Fig. 19. Profiles of four rapid bursts with different durations observed from Tenma

We indeed found that the structure is nearly identical, if the time axis is properly scaled for each burst. In other words, the decay structure of the rapid bursts is time-scale invariant and can be expressed by a single function  $F(t/\tau)$ , with  $\tau$  a characteristic time for each burst [21][23]. This is clearly demonstrated by the composite profiles in Fig. 20, which are constructed by superposing a number of bursts after scaling the time axis. The characteristic time is determined by cross-correlation between bursts. From this figure, we see that the time-scale invariance of the decay structure holds for a remarkably wide range of the characteristic time, over a dynamic range of at least thirty. Moreover, as noticed in the figure, the fine detail is not lost by superposing many bursts. This fact clearly indicates that the structure is intrinsic and fixed in the system. This conclusion is further strengthened by the observed fact that the structure is unaltered by a change in the peak luminosity as well as the time-averaged luminosity (accretion rate) which varied by as much as a factor of two between the 1983 and 1984 activities.

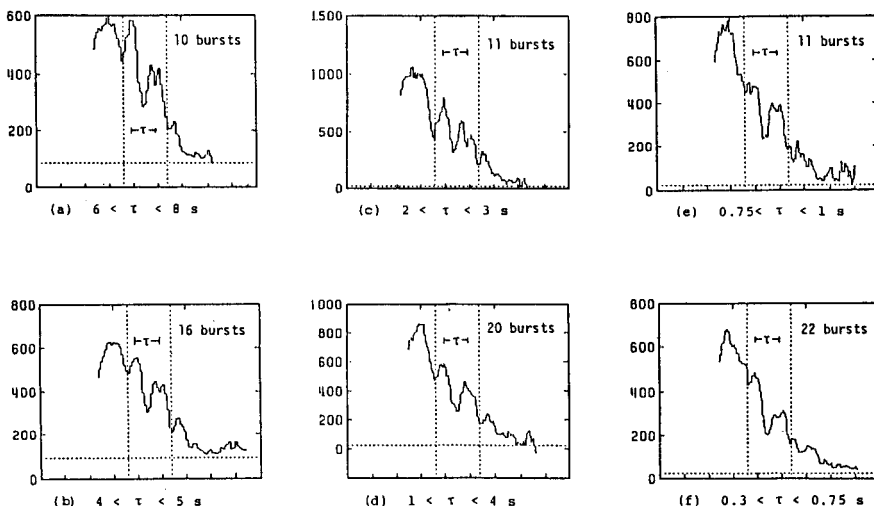


Fig. 20. Composite profiles of rapid bursts for different ranges of characteristic time

If the luminosity at a given time during a burst were determined by the accretion rate at that time, the above result would imply the presence of an extremely sophisticated mechanism that controls the flow rate according to a prescribed form  $F(t/\tau)$ . One might speculate that the corresponding structure was already formed in the accretion disk (e.g., concentric rings). It is, however, very hard to explain the fact that the structure is constant for a wide range of  $\tau$  and is not influenced by the changes in accretion rate. This result makes the Rapid Burster even more enigmatic than before.

#### I-4. Black-Hole Candidate Sources

There are three X-ray sources thus far for which the mass lower limit of the compact object exceeds  $3M_{\odot}$ , and hence are suspected to be black holes. These are Cyg X-1 ( $>9M_{\odot}$ ) [24], LMC X-3 ( $>7M_{\odot}$ ) [25] and LMC X-1 ( $>3M_{\odot}$ ) [26]. In addition, two more sources are considered black-hole candidates, because they exhibit characteristics similar to those of Cyg X-1. These sources are GX339-4 and Cir X-1.

The following distinct characteristics of Cyg X-1 have been suspected as possible signatures of black-hole sources (for a review of Cyg X-1, e.g., [27]):

- (i) the existence of rapid and chaotic intensity fluctuations, or flickering, and
- (ii) two distinct states; (a) a high-intensity state (ultrasoft spectrum + hard tail) and (b) a low-intensity state (hard, power-law spectrum).

Cyg X-1 undergoes flickering over a wide range of time scale down to 1 msec or even shorter. The flickering is much more pronounced in the low-intensity state, and hence is considered to be intrinsic to the power-law component. GX339-4 also exhibits similar flickering in its low-intensity (hard, power-law spectrum) state. Cir X-1 shows a rapid variability as well, though the nature of the variation appears somewhat different from the other two sources.

Flickering of time scales as short as 1 msec is certainly a unique phenomenon, yet the physics involved is entirely unknown. However, flickering as a signature of a black hole has come into question. We discovered prominent flickering in the transient source X0331+53 [28] as shown in Fig. 21, which is very similar to Cyg X-1. This source was subsequently found to be an X-ray pulsar from an EXOSAT observation [29]. Thus, unless a black hole source could pulsate, flickering is not necessarily a black-hole signature.

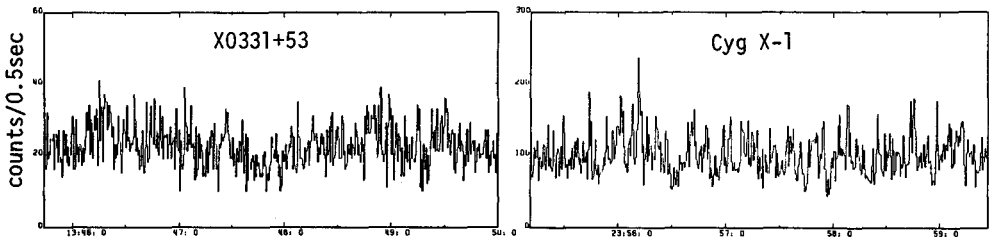


Fig. 21. Flickering of X0331+53 observed from Tenma and that of CygX-1 for comparison

As regards the existence of high- and low-intensity states, GX339-4 and Cir X-1 exhibit similar behavior to Cyg X-1. Figure 22 shows the spectra for the two states of Cir X-1 observed from Tenma. The occurrence of the two states is interpreted qualitatively as follows. When the accretion rate is high enough, the accretion disk will be optically thick, from which a soft spectrum is expected. On the other hand, when the accretion rate is low, the disk will become optically thin, and Compton up-scattering will form a hard, power-law spectrum. As discussed earlier, the spectrum of the burst source X1608-52 changed from a thermal spectrum to a power-law spectrum when the accretion rate decreased. Although X1608-52 is a neutron-star source, this change may be similar in nature to the two states discussed above.

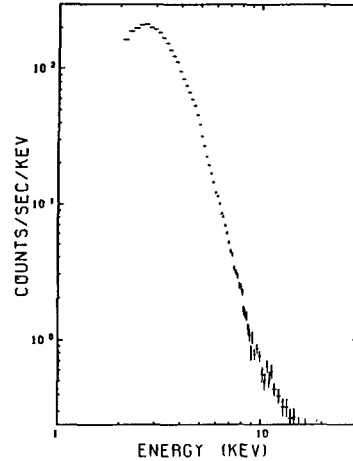
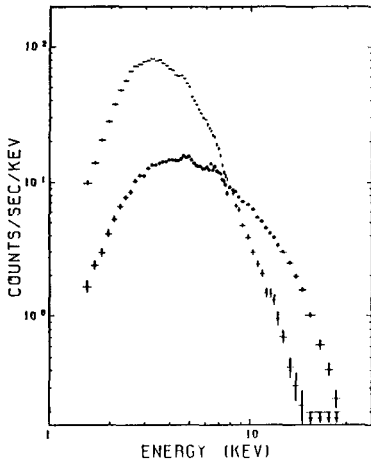


Fig. 22. Spectra for two states of Cir X-1

Fig. 23. Ultrasoft spectrum of GX339-4

Additionally, all these black-hole candidates, selected either from the mass lower limit or because of characteristics similar to Cyg X-1, exhibit an ultrasoft spectrum, at least for some time, which is significantly softer than those of most low-mass binary sources. For an example, Fig. 23 shows an ultrasoft spectrum of GX339-4 we observed [30]. WHITE and MARSHALL [31] suggest that the ultrasoft spectrum may be a signature of a black hole.

In fact, an ultrasoft spectrum is expected for a black hole source, based on the discussions in Section I-2. Since a black hole is generally considered to possess no magnetic field, the accretion disk can extend close to the Schwarzschild radius. The essential difference in the accretion flow for a black hole compared to a neutron star is the absence of a solid surface. Hence, the spectrum of an accreting black hole would lack the 2-keV blackbody component. Indeed, the observed ultrasoft spectra from the black hole candidates are very similar to the softer component of the low-mass binary sources, which is considered to be the emission from an optically-thick accretion disk. This picture explains, at least qualitatively, the nature of the ultrasoft spectrum for black-hole sources. In this respect, there are several more sources that show similarly ultrasoft spectra [31] and are therefore worth paying attention to. These sources include Cyg X-3, X0620-00, X1630-47 and X1957+11.

In addition, the ultrasoft spectra from black-hole candidate sources are often accompanied by a distinct, power-law tail, as noticeable for instance in Fig. 23. This feature can be explained in terms of an additional component which is produced by Compton up-scattering of part of the photons from the optically-thick disk within the optically-thin, hot inner disk.

## II. X-Ray Bursts

In this section, we shall discuss exclusively Type I X-ray bursts according to the designation of HOFFMAN et al. [18], which are qualitatively different from Type II bursts discussed earlier. An X-ray burst is a violent phenomenon observed from many galactic sources. A typical example is shown in Fig. 24, although there are a large variety of burst profiles. At present, about thirty sources are known to produce bursts. They are sharply concentrated towards the galactic center, and indeed fourteen burst sources, about one half, cluster within only 10 degrees of the galactic center. About ten burst sources are found in globular clusters. Sufficient evidence exists to believe that the burst sources are low-mass binaries with an accreting neutron star (for a general review of X-ray bursts, see e.g., [2][32]).

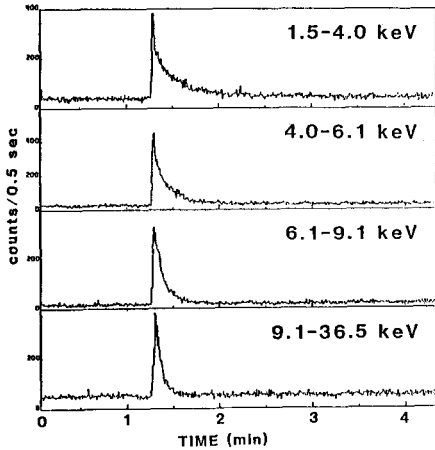


Fig. 24. Profile of an X-ray burst from X1636-53 displayed in four different energy bands

X-ray bursts are currently interpreted as nuclear shell flashes occurring on the neutron star surface [33]. The variation in emission during a burst follows that expected from a cooling blackbody. The size of the blackbody indeed turned out to be the right order of magnitude for a neutron star [34][35][36]. As discussed in what follows, X-ray bursts provide us with a useful means to "measure" neutron stars. In fact, X-ray bursts have been the subject of intensive study with Hakucho and Tenma. In particular, the gas scintillation proportional counters of Tenma enable us to obtain spectral information of bursts in much more detail than previously possible.

#### II-1. Blackbody Spectrum and Apparent Blackbody Radius

Figure 25 shows examples of burst spectra measured at two different temperature values. They are indeed in very good agreement with blackbody spectra, except for a slight high-energy excess above 10 keV. This high-energy excess is considered to arise from Comptonization as discussed in Section I-2. From the measured blackbody temperature  $T_b$  and the observed bolometric flux  $F_X$ , one derives the apparent blackbody radius  $r_b$  by

$$L = 4\pi D^2 F_X = 4\pi r_b^2 \sigma T_b^4 \quad (4)$$

where  $D$  is the distance to the source.

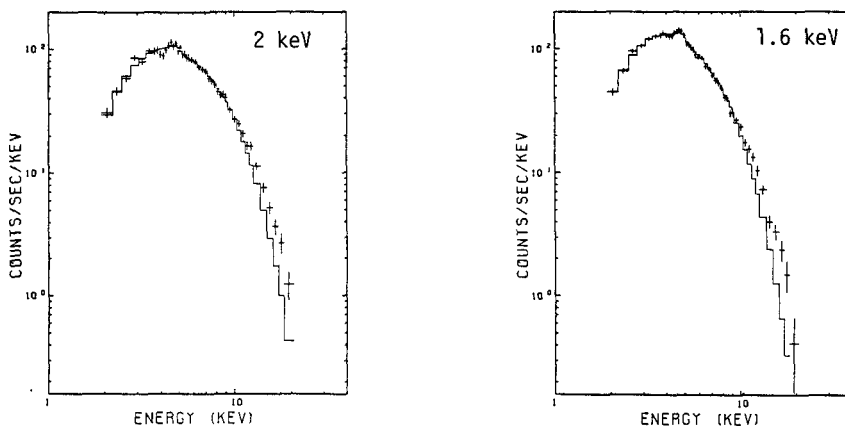


Fig. 25. Spectra of burst from X1636-53 at two temperature values (Tenma) Histograms are the best-fit blackbody spectra.

We are interested in relating  $r_b$  to the actual neutron star radius  $r_0$ . To do so, the following considerations are necessary. First, we need to know if a burst covers the entire neutron star surface so that the emission is isotropic. Observed results indeed support that every burst covers the entire neutron star surface. For a given burst source, the apparent blackbody radii are always the same for all bursts within the uncertainties, despite the large variation in the burst peak flux and burst size from burst to burst [37][38]. This fact works against a partial surface coverage of a burst. Furthermore, the observed blackbody radii for several burst sources located near the galactic center are found to be all about 10 km [39]. This result even supports similarity in size between the neutron stars in the burst sources.

The second point is that  $T_b$  is the color temperature, which is not equal to but higher than the effective temperature. During a burst, the opacity of the neutron star atmosphere is predominantly due to electron scattering, and the flux is reduced by an emissivity factor  $\epsilon$  as compared to the blackbody emission [40]. Taking into account the general relativistic effect,

$$4\pi D^2 F_X = 4\pi r_0^2 g^{-2} \sigma T_b^4 \epsilon \quad (r_b = r_0 g^{-1} \epsilon^{1/2}), \quad (5)$$

where

$$g^2 = 1 - \frac{2GM}{c^2 r_0}. \quad (6)$$

Figure 26 shows the relation between  $r_b$  and  $T_b$  for a number of bursts observed from X1636-53 [41]. This diagram clearly indicates the temperature-dependence of  $\epsilon$ , which increases with decreasing temperature.

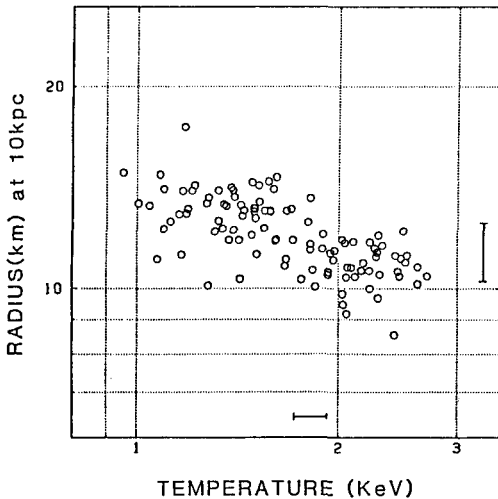


Fig. 26. Distribution of  $r_b$  at various values of  $T_b$ , derived according to Eq. 4 for a number of bursts from X1636-53

If  $\epsilon$  and  $g$  are known, the mass  $M$  and radius  $r_0$  can be determined from Eq. 5 and 6, provided that the distance  $D$  is known. The evaluation of the emissivity factor  $\epsilon$  by solving radiative transfer, taking into account the Compton effect, is presently in progress [42][43]. Preliminary results already show that the effect of electron scattering is quite significant.

Since X-ray bursts are the phenomenon on a neutron star surface, a significant general relativistic effect is expected. If a gravitational redshift is measured, the  $g$ -value is directly obtained from the redshift factor  $(1+z)=1/g$ . Moreover, the  $g$ -value gives the mass to radius ratio  $M/r_0$  of the neutron star from Eq. 6, independent of the source distance.

## II-2. Absortion Line

A significant spectral feature was discovered in the burst spectra from a Tenma observation, which is most probably a redshifted absorption line [44]. Among a total of twelve bursts from X1636-53 observed in 1983, the largest three bursts and one smaller burst revealed a similar absorption feature during the burst decay, as shown in Fig. 27. In these four cases, the observed profile agrees with an absorption line, and the line energy is consistent in all cases with a value of 4.1 keV. The equivalent widths of the absorption line ranged between 100 and 200 eV. Detection of absorption lines in other bursts, although several were suggestive, were not statistically significant. A similar absorption line at about 4 keV was also detected in a burst from another burst source X1608-52.

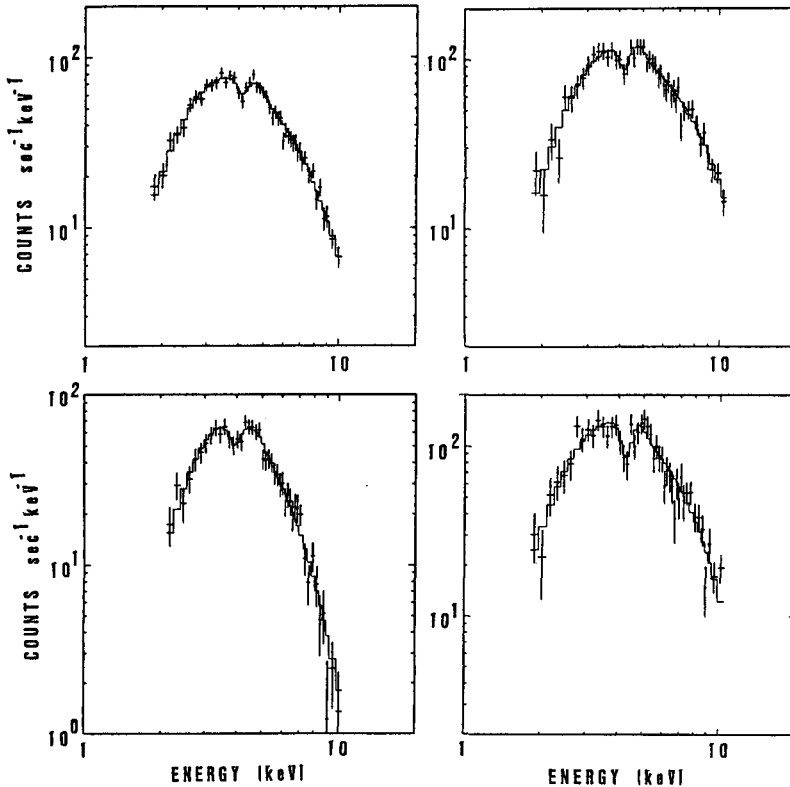


Fig. 27. Absorption lines observed in the decay of four different bursts from X1636-53. Histograms are the best-fit time-averaged blackbody spectra including a line.

We consider it most plausible that the absorption is caused by iron, the most abundant heavy element in the accreted matter. If so, the observed line energy of 4.1 keV gives a redshift factor  $(1+z)=1.61 \pm 0.04$ , assuming the helium-like ionization state and a laboratory line energy of 6.7 keV. If the redshift were interpreted as due to a gravitational effect, the corresponding  $g$ -value is  $0.62 \pm 0.02$ . This small  $g$ -value has a serious impact on current theoretical models of stable neutron stars [45]. As shown in Fig. 28, the resulting value of  $M/r_0$  turns out to be uncomfortably large for all available models. Alternatively, FUJIMOTO [46] proposed the idea that the observed redshift may be the transverse Doppler effect caused by the accreted matter circulating around the neutron star at high speed. Obviously, more observational as well as theoretical work is required in order to fully interpret nature of the absorption line. In any event, the observed absorption line contains information of great importance.

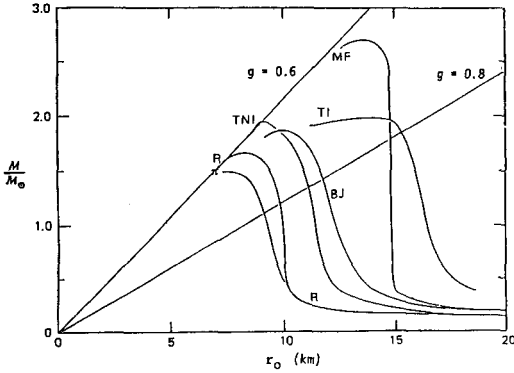


Fig. 28. Mass vs. radius relations for stable neutron star models. Two lines corresponding to  $g=0.6$  and  $0.8$  are also indicated.

II-3. Burst Peak Luminosity

We recognized for some time that burst peaks are often exceedingly luminous. Figure 29 shows the distribution of the peak flux as observed by Hakucho from five burst sources which are all within six degrees of the galactic center [39]. In view of the sharp concentration of burst sources toward the galactic center, most of the five sources will be within 1 kpc of the galactic center, for an assumed distance of 8 kpc. The observed peak-flux values are compared with the Eddington limit. The Eddington limit luminosity  $L_E$  for a distant observer is given by

$$L_E = \frac{4\pi c GM}{\kappa_0(1+X)} g = 1.59 \times 10^{38} \left(\frac{M}{1.4M_\odot}\right) \left(\frac{1.7}{1+X}\right) \left(\frac{g}{0.76}\right) \text{ ergs/sec} \quad (7)$$

where  $\kappa_0(1+X)$  is the Thomson scattering opacity and  $X$  the mass fraction of hydrogen. The flux value corresponding to the Eddington limit is indicated in the figure, assuming the cosmic abundance of elements, for a neutron star of  $1.4 M_\odot$  and  $10 \text{ km}$  radius ( $g=0.76$ ) located at  $8 \text{ kpc}$  distance. The maximum peak-flux values observed are all in excess of this Eddington limit by factors ranging from 2 to 6. Similarly large discrepancies have been reported for the bursts from the globular clusters NGC6624 [47] and Trz 2 [48].

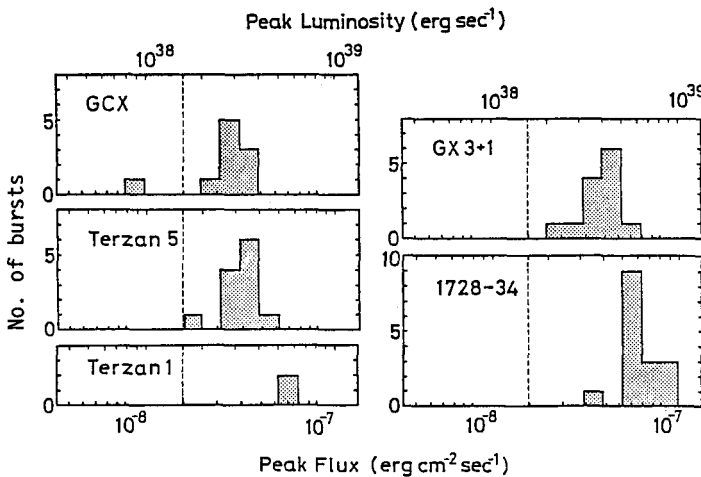


Fig. 29. Distribution of the peak flux of bursts from five sources within six degrees of the galactic center. The Eddington limit given by Eq. 7 is shown by dashed line.

This apparent "super-Eddington" problem has been a controversial issue. Some attempts have been made to explain it in terms of dynamical processes [33]. However, X-ray bursts do not seem to involve large-scale dynamical process, because the rise time of a burst is of the order of one second, orders of magnitude larger than the dynamical time scales on a neutron star. Therefore, the radiation during a burst is regarded to be quasi-stationary, and hence the peak luminosity is expected to saturate at the Eddington limit. If bursts are indeed nuclear shell flashes, the theoretical models do not predict peak luminosities significantly in excess of the Eddington limit [49][50].

Recently, there has been an increasing amount of supporting evidence that the burst peak luminosity indeed saturates at the Eddington limit. A result from Tenma reveals the detail when the burst peak flux reached the upper bound [41]. Figure 30 shows three bursts from X1636-53 with the largest peak flux among twelve observed. They exhibit a flat top for a few seconds all at the same flux value within statistical uncertainties. Furthermore, the blackbody temperature as well as the apparent blackbody radius undergo a large excursion during the flat top. In fact, the observed feature is quite explicable in terms of saturation at the Eddington limit. When the luminosity reaches the Eddington limit, the radiation pressure expands the atmosphere and consequently temperature decreases. As the radiation pressure starts to decline, the atmosphere shrinks back gradually and temperature rises accordingly. During this phase, the luminosity stays constant at the Eddington limit. This is exactly what is observed. Very long bursts with a precursor in which the peak luminosity remained constant for more than 100 seconds are interpreted in the same way [51][52]. The above results are convincing for the burst peak saturation due to the Eddington limit.

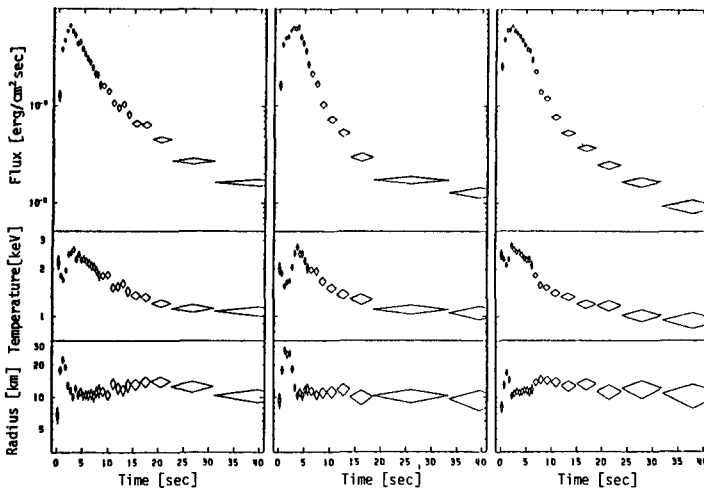


Fig. 30. Three bursts with the largest peak flux among those observed from Tenma

Bolometric flux, blackbody temperature and apparent blackbody radius are shown, respectively.

SUGIMOTO et al. [53] suggest that the hydrogen envelope may be ejected in an energetic burst and the saturating peak luminosity corresponds to the Eddington limit for helium-rich atmosphere ( $X=0$ ), which is larger by a factor of 1.7 than that for cosmic abundances. Even if this were the case, the discrepancy is not resolved.

EBISUZAKI et al. [54] compiled the largest peak flux for each of the observed burst sources available so far, and estimated a distance to each based on the assumption that the peak luminosity is at the Eddington limit for a helium-rich atmosphere. A model neutron star of  $1.4M_{\odot}$  and 10 km radius was assumed. They found that the distribution of the estimated locations is centered at about 6 kpc from the sun. Since not all of the adopted bursts were necessarily saturated, this distance may become even smaller. Unless the neutron star mass is significantly larger than  $1.4M_{\odot}$ , this might be taken as an indication that the distance to the galactic center is not much more than 6 kpc.

#### II-4. Nuclear Fuel Reservoir

According to nuclear shell flash model of X-ray bursts, mass accretion supplies the required nuclear fuel. Since the same accreted matter accounts for the persistent emission, the ratio of the persistent luminosity to the time-averaged burst luminosity ( $\alpha$ ) is equal to the ratio of the gravitational energy to the nuclear energy released per unit mass. The  $\alpha$ -value is expected to be about 100 for helium flash, and is no smaller than 20 even if hydrogen burning is included. In most cases, the observed  $\alpha$ -values are of the order of 100, although we sometimes find  $\alpha$ -values as small as 20.

In general, nuclear shell flash models predict that a burst completely exhausts the then available nuclear fuel. It usually takes an hour or longer before a sufficient amount of matter for a burst accumulates on the neutron star. Several cases have been observed where two or more bursts occurred in succession with separations of only several minutes [55][56][57]. An example is shown in Fig. 31, observed from X1608-52. For these events, the  $\alpha$ -values were of the order of unity. In other words, the time interval was far too short for enough fuel to accumulate for the next burst. It is therefore an avoidable conclusion that there must be a reservoir of nuclear fuel on the neutron star surface.

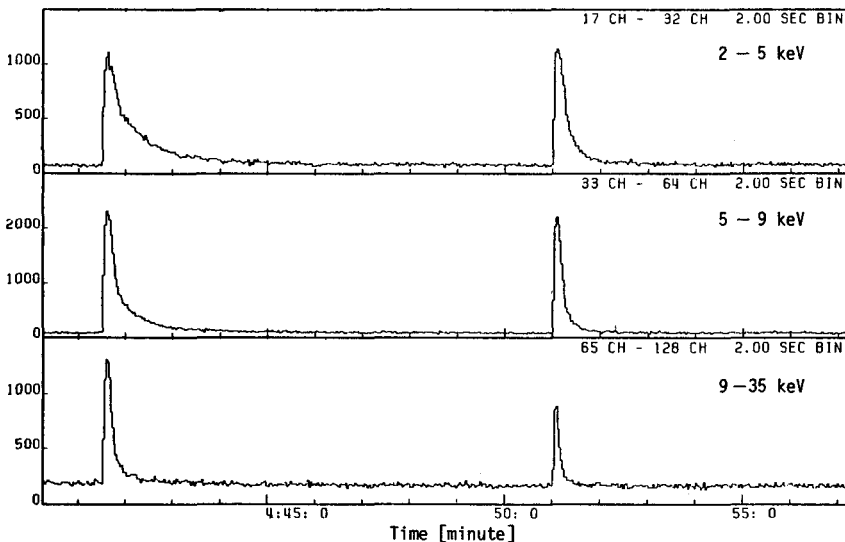


Fig. 31. Two bursts from X1608-52 with ten minutes separation, observed from Tenma

It cannot be that a part of the neutron star surface produced a burst leaving other parts of the surface for the next burst, because both of the two successive bursts observed from the Trz 5 source showed the same blackbody radius as those for other well-separated bursts from the same source [57]. AYASLI and JOSS [58] indicate that some amount of hydrogen can be left unused in a burst. This may provide the fuel for the next burst. However, a big question is how this matter establishes a critical condition to trigger a burst within a time as short as several minutes. No satisfactory explanation has yet been obtained. Although nuclear shell flash models have been very successful in explaining basic characteristics of X-ray bursts, this issue still remains as a critical problem to be solved in future.

## References:

1. N.E. White, J.H. Swank and S.S. Holt: *Ap. J.*, 270, 711 (1983)
2. P.C. Joss and S.A. Rappaport: *Ann. Rev. Astr. Ap.*, 22, 537 (1984)
3. H. Inoue, Y. Ogawara, T. Ohashi et al.: *Publ. Astr. Soc. Japan*, 36, 709 (1984)
4. K. Mitani, M. Matsuoka, K. Makishima et al.: *Ap. Space Sci.*, 103, 345 (1984)
5. J. Truemper, W. Pietsch, C. Reppin et al.: *Ap. J. (Letters)*, 219, L105 (1978)
6. T. Ohashi, H. Inoue, K. Koyama et al.: *Publ. Astr. Soc. Japan*, 36, 699 (1984)
7. S.H. Pravdo: "X-Ray Astronomy" ed. Baiy and Peterson (Pergamon Press, 1979) p.169
8. F. Makino, D.A. Leahy and N. Kawai: *Proc. 18th ESLAB Symposium*, Scheveningen (1985)
9. R. Hoshi: *Publ. Astr. Soc. Japan*, 36, 785 (1984)
10. K. Mitsuda, H. Inoue, K. Koyama et al.: *Publ. Astr. Soc. Japan*, 36, 741 (1984)
11. M. Itoh: *ISAS RN289* (1985)
12. J. Nishimura, K. Mitsuda and M. Itoh: in preparation (1985)
13. K. Mitsuda and Y. Tanaka: *Proc. NATO Advanced Workshop on the Evolution of Galactic X-Ray Binaries*, Tegernsee, in press (1985)
14. K. Suzuki, M. Matsuoka, H. Inoue et al.: *Publ. Astr. Soc. Japan*, 36, 761 (1984)
15. J.C. Raymond and B.W. Smith: *Ap. J. Suppl.*, 35, 419 (1977)
16. N.E. White and K.O. Mason: *Proc. 18th ESLAB Symposium*, Scheveningen (1985)
17. W.H.G. Lewin, J. Doty, G.W. Clark et al.: *Ap. J. (Letters)*, 207, L95 (1976)
18. J.A. Hoffman, H.L. Marshall and W.H.G. Lewin: *Nature*, 271, 630 (1978)
19. H. Inoue, K. Koyama, K. Makishima et al.: *Nature*, 283, 358 (1980)
20. H. Kunieda, Y. Tawara, S. Hayakawa et al.: *Publ. Astr. Soc. Japan*, 36, 807 (1984)
21. N. Kawai: Ph.D. Thesis Univ. of Tokyo (1985)
22. Y. Tawara, S. Hayakawa, H. Kunieda et al.: *Nature*, 299, 38 (1982)
23. Y. Tawara, N. Kawai, Y. Tanaka et al.: submitted to *Nature* (1985)
24. J.N. Bahcall: *Ann. Rev. Astr. Ap.*, 16, 241 (1978) and references therein
25. A.P. Cowley, D. Crampton, J.B. Hutchings et al.: *Ap. J.*, 207, 118 (1983)
26. J.B. Hutchings, D. Crampton and A.P. Cowley: *Ap. J. (Letters)*, 275, L43 (1983)
27. M. Oda: *Space Sci. Rev.*, 20, 757 (1977)
28. Y. Tanaka and the Tenma team: *IAU Circular No.3891* (1983)
29. L. Stella, N.E. White, J. Davelaar et al.: *Ap. J. (Letters)*, 288, L45 (1985)
30. K. Makishima, K. Maejima, K. Mitsuda et al.: submitted to *Ap. J.* (1985)
31. N.E. White and F.E. Marshall: *Ap. J.*, 281, 354 (1984)
32. W.H.G. Lewin and P.C. Joss: "Accretion-Driven Stellar X-Ray Sources" ed. Lewin and van den Heuvel (Cambridge University Press, 1983) p.41
33. F. Melia: *This Colloquium* (1985)
34. J.H. Swank, R.H. Becker, E.A. Boldt et al.: *Ap. J. (Letters)*, 212, L73 (1977)
35. J.A. Hoffman, W.H.G. Lewin and J. Doty: *Ap. J. (Letters)*, 217, L23 (1977)
36. J. van Paradijs: *Nature*, 274, 650 (1978)
37. W.H.G. Lewin, J. van Paradijs, L. Cominsky et al.: *M.N.R.A.S.*, 193, 15 (1980)
38. T. Ohashi, H. Inoue, K. Koyama et al.: *Ap. J.*, 258, 254 (1982)
39. H. Inoue, K. Koyama, K. Makishima et al.: *Ap. J. (Letters)*, 250, L71 (1981)
40. J. van Paradijs: *Astr. Ap.*, 107, 51 (1982)
41. H. Inoue, I. Waki, K. Koyama et al.: *Publ. Astr. Soc. Japan*, 36, 831 (1984)
42. R.A. London, R.E. Taam and W.H. Howard: *Ap. J. (Letters)*, 287, L27 (1984)
43. T. Ebisuzaki and K. Nomoto: "Japan-US Seminar on Galactic and Extragalactic Compact X-Ray Sources" ed. Tanaka and Lewin (ISAS, 1985) p.101
44. I. Waki, H. Inoue, K. Koyama et al.: *Publ. Astr. Soc. Japan*, 36, 819 (1984)
45. G. Baym and C. Pethick: *Ann. Rev. Astr. Ap.*, 17, 415 (1979)
46. M.Y. Fujimoto: *Ap. J. (Letters)*, 293, L19 (1985)
47. G.W. Clark, J.G. Jernigan, H. Bradt et al.: *Ap. J. (Letters)*, 207, L105 (1976)
48. J.E. Grindlay, H.L. Marshall, P. Hertz et al.: *Ap. J. (Letters)*, 240, L121 (1980)
49. T. Ebisuzaki, T. Hanawa and D. Sugimoto: *Publ. Astr. Soc. Japan*, 35, 17 (1983)
50. M. Kato: *Publ. Astr. Soc. Japan*, 35, 33 (1983)
51. Y. Tawara, T. Kii, S. Hayakawa et al.: *Ap. J. (Letters)*, 276, L41 (1984)
52. W.H.G. Lewin, W.D. Vacca and E.M. Basinska: *Ap. J. (Letters)*, 277, L57 (1984)
53. D. Sugimoto, T. Ebisuzaki and T. Hanawa: *Publ. Astr. Soc. Japan*, 36, 839 (1984)
54. T. Ebisuzaki, T. Hanawa and D. Sugimoto: *Publ. Astr. Soc. Japan*, 36, 551 (1984)
55. W.H.G. Lewin, J.A. Hoffman, J. Doty et al.: *M.N.R.A.S.*, 179, 83 (1976)
56. T. Murakami, H. Inoue, K. Koyama et al.: *Publ. Astr. Soc. Japan*, 32, 543 (1980)
57. H. Inoue, K. Koyama, F. Makino et al.: *Publ. Astr. Soc. Japan*, 36, 855 (1984)
58. S. Ayasli and P.C. Joss: *Ap. J.*, 256, 637 (1982)

Blandford: You decomposed the neutron star spectrum into two components that have rather similar temperatures. Isn't this rather surprising when you would expect less power to be radiated from a larger area in the outer disk and more power to be radiated from a smaller area on the surface of the neutron star?

A:  $T_{in}$  is the temperature at the inner limit of the optically thick accretion disk. Comparable values for  $T_{in}$  and  $T_b$  can be understood because the estimated radius of the inner edge is only a few times the neutron star radius.

Ogelman: With regard to the two-component fits, would you not expect the component appropriate to the neutron star surface to have a higher luminosity in comparison to the disk component; and is this what you see?

A: Yes, we expect the emission from the neutron star surface to be greater than that from the optically-thick disk, since the internal energy of the optically-thin disk would eventually be carried onto neutron star. The observed ratio is generally greater than unity. However, the ratio can be smaller than unity, because it depends on the inclination of the accretion disk.

Meyer: You mentioned the constancy of the pattern in the Rapid Burster bursts though energy of burst and duration vary. How does the time scale correlate with the energy?

A: The time scale of the decay structure is primarily proportional to the size (integrated energy) of each burst. However, this relation may only be apparent, because the size is proportional to the time scale.

Krolik: Does the shape of the 4.1 keV absorption feature seen in X-ray bursts change during the burst?

A: We are unable to resolve such a detail, except that the line was significant only during a portion of the bursts and not throughout.

Shull: Since the Fe line is in absorption (and doesn't involve fluorescence yields), you might expect Si and S lines. Are they there? What about the Fe K-continuum edge?

A: No. Technically, we could hardly detect Si or S lines, when redshifted as much as observed for Fe line. We do not see the Fe K-edge significantly, and the upper limit for the Fe K-edge sets the upper limit of the Fe column which is responsible for the absorption line.

Bath: Does the Rapid Burster show any indications of Eddington limited effects found in other burst sources, or is it of too low a luminosity?

A: None of many Type I bursts we observed from the Rapid Burster showed an evidence of photospheric expansion associated with the Eddington saturation. We think they are below the Eddington limit.

McCray: In the determination of the distance of the galactic center from the brightness of X-ray bursts, are all X-ray bursters included in the sample, or only those bursters showing evidence of photospheric expansion?

A: Ebisuzaki et al. simply employed the largest peak flux of observed bursts from each source, and not all of them had evidence for a photospheric expansion.

Blandford: It might be worth pointing out that some contemporary determinations of the distance to the galactic center give values less than the "standard" 10 kpc. In particular, a determination based on the distribution of globular clusters (Frank and White) gives 7 kpc.